INSTITUTE OF PHYSICS PUBLISHING JOURNAL OF PHYSICS D: APPLIED PHYSICS

J. Phys. D: Appl. Phys. **38** (2005) 2253–2257 doi:10.1088/0022-3727/38/13/025

# Influence of Ce doping on leakage current in $Ba_{0.5}Sr_{0.5}TiO_3$ films

**S Y Wang[1], B L Cheng[1,3], Can Wang[1], S A T Redfern[2], S Y Dai[1], K J Jin[1], H B Lu[1], Y L Zhou[1], Z H Chen[1] and G Z Yang[1]**

[1] Beijing National Laboratory for Condensed Matter Physics, Institute of Physics, Chinese Academy of Sciences, Beijing 100080, People's Republic of China
[2] Department of Earth Science, University of Cambridge, Downing Street, Cambridge, CB2 3EQ, UK

E-mail: blcheng@aphy.iphy.ac.cn

Received 6 January 2005, in final form 17 April 2005
Published 17 June 2005
Online at stacks.iop.org/JPhysD/38/2253

**Abstract**

Undoped and Ce-doped $Ba_{0.5}Sr_{0.5}TiO_3$ (BST) thin films were prepared by pulsed-laser deposition onto a Nb-doped $SrTiO_3$ (STON) substrate. The Ce concentration, ranging from 0.5 to 1.0 at.%, was found to have a strong influence on the electric properties of films at room temperature. We find that, with a positively biased Pt electrode, the leakage current controlled by BST/STON interface can be described by a space-charge-limited-current model. When the Pt electrode is negatively biased, the leakage current controlled by the BST/Pt interface can be explained by the Schottky emission mechanism. In both cases the Ce-doped BST thin films exhibited a lower leakage current ($1.2 \times 10^{-4}$ and $5.0 \times 10^{-5}$ versus $3.4 \times 10^{-2}$ A cm$^{-2}$ at 450 kV cm$^{-1}$; $4.0 \times 10^{-4}$ and $4.0 \times 10^{-5}$ versus $6.2 \times 10^{-3}$ A cm$^{-2}$ at $-450$ kV cm$^{-1}$) than undoped BST films. The reduction of the leakage current is ascribed to the effect of acceptor $Ce^{3+}$ doping, determined by x-ray photoelectron spectroscopy measurement.

(Some figures in this article are in colour only in the electronic version)

## 1. Introduction

$Ba_{1-x}Sr_xTiO_3$ (BST) thin films have recently received considerable attention since they are promising candidates for application in tunable microwave devices and in dynamic random access memories (DRAM) [1–3]. High electric insulation with low leakage current is one of the crucial factors in the commercial application of such film [4, 5]. The leakage current behaviours have been extensively investigated. Thus far, leakage mechanisms that have been proposed include Schottky emission [6], modified Schottky emission [2], tunnelling [4], space-charge-limited current (SCLC) [7] and Poole–Frenkel emission [8]. It has been suggested that interface contamination, annealing conditions and dopant have a major effect on the electric properties of BST thin film [4–6]. Ahn *et al* [4] observed a decrease of leakage current associated with acceptor (Mn, Ni) doping in a Pt/BST/Pt capacitor. They proposed that the suppression of leakage current in the doped capacitor was caused by an expansion of the depletion layer width, which decreases the effect of tunnelling. Copel *et al* [9] investigated the effects of acceptor Mn doping on the electric properties of BST thin films using x-ray photoemission spectroscopy. They presented evidence that acceptor-doped films show an increased barrier to thermonic emission of electrons from Pt contacts to the BST. Cole *et al* observed that rare-earth element of 1.0 at% La-doped BST film exhibited higher resistivity than that of undoped films. On the other hand, as reported by Sedlar *et al* , [10, 11] the rare-earth element Ce dopant can increase BST dielectric permittivity for thin films prepared by spin coating. Such a kind of variation of BST permittivity is useful for the application of DRAM. We have also noted that the rare-earth element Ce can have a modifying effect on the size of BST lattice, which is helpful for well accommodation between the BST thin film and MgO substrates. Therefore, we have investigated the influence of the Ce dopant on BST thin films prepared by pulsed-laser deposition (PLD). In previous studies leakage was investigated in a symmetric Pt/BST/Pt capacitor, and

[3] Author to whom any correspondence should to be addressed.

the leakage mechanism controlled by the BST/Pt interface was independent of bias polarity [4–6, 9]. In our recent works, [12, 13] we found that in a Pt/BST/Nb-doped $SrTiO_3$ (STON) capacitor the leakage current showed different leakage mechanisms for different bias polarity, and we carried out a study of Co-doping dependence on the leakage current in the positive electric field region. In this paper, we will demonstrate the suppression of leakage current by Ce doping in an unsymmetrical Pt/BST/STON capacitor. In particular, the valence state of Ce ions has been investigated by x-ray photoelectron spectroscopy (XPS) to explore the origins of the suppression of leakage current.

## 2. Experimental

The undoped and Ce-doped BST (at% Ce = 0.5,1.0) ceramic targets were prepared with conventional solid-state synthesis from oxides. Before deposition, the deposition chamber was evacuated to a background pressure of $1 \times 10^{-3}$ Pa, and then pressurized to 20 Pa by introducing $O_2$. For PLD, a XeCl excimer laser beam (308 nm, 20 ns, 4 Hz and 2 J $cm^{-2}$) was used as the laser source. The ceramic target was mounted on a rotating holder, 40 mm from the STON substrates, which were held at 750°C. After the deposition, the BST films were annealed at the same temperature of 750°C for 10 min under an oxygen pressure of 500 Pa. The thickness of the BST films was found to be about 200 nm, using a surface profile measuring system (DEKTAK, USA).

The crystalline phase and structure of the BST films were analysed by x-ray diffraction (XRD) employing CuK$\alpha$ radiation. Figure 1 shows the XRD $\theta$–$2\theta$ scan of the BST/STON heterostructures. The results indicate that neither impurity phases nor out-of-plane disorientation was observed for the films. Lattice parameters of the BST films, calculated from the position of (002) peaks, are observed to increase from 3.999 Å to 4.002 Å and 4.025 Å with Ce concentration. These data indicate that Ce ions have dissolved into the BST lattice, resulting in the expansion of the BST unit cell. Because the ionic radii of Ce ions ($Ce^{3+}$ = 1.01 Å, $Ce^{4+}$ = 0.87 Å) are larger than that of $Ti^{4+}$ (0.61 Å), and smaller than that of $Ba^{2+}$ (1.35 Å) or $Sr^{2+}$ (1.18 Å), the increased lattice parameter implies that Ce ions substitute onto the B site of the $ABO_3$-type perovskite, BST.

For electric measurements, Pt-top electrodes with a diameter of 0.2 mm were deposited using a shadow mask onto the BST films under a pressure of $1 \times 10^{-3}$ Pa at room temperature. Measurements were made using an RT-6000S ferroelectric test system. The bias voltage is defined as positive and negative when positive and negative voltage is applied to top Pt electrode, respectively.

## 3. Results and discussion

The influence of Ce-doping on the current density versus electric field ($J$–$E$) characteristics of BST films is shown in figure 2. The leakage current in the undoped BST film is remarkably reduced upon addition of Ce at each given electric field. For example, at an electric field of 450 kV $cm^{-1}$, the leakage current density of $3.4 \times 10^{-2}$ A $cm^{-2}$ in undoped BST film decreases to $5.0 \times 10^{-5}$ A $cm^{-2}$ in 1.0 at% Ce-doped BST film. On the other hand, at a field of −450 kV $cm^{-1}$, the leakage current of $6.2 \times 10^{-3}$ A $cm^{-2}$ decreases to $4.0 \times 10^{-5}$ A $cm^{-2}$ for the same level of doping. Such a phenomenon is consistent with previous reports stating that Ni, Mn and MgO dopants significantly decrease the leakage current in a Pt/BST/Pt capacitor [4, 9]. Another notable feature in figure 2 is that in different electric field regions, the Ce-doping dependence of leakage current shows different characteristics. The bias polarity dependence of the $J$–$E$ characteristics reveals that different leakage mechanisms operate in the positive and negative bias region. To clarify the leakage mechanisms, the $J$–$E$ data have been investigated further.

At a high electric field, with a negatively biased Pt electrode, the Schottky equation can be used to analyse the leakage current data. The current density $J$ is then expressed as [3, 6]

$$J = A^* T^2 \exp\left(\frac{-q\left(\phi_B - \sqrt{qE/4\pi\varepsilon_0\varepsilon}\right)}{kT}\right), \qquad (1)$$

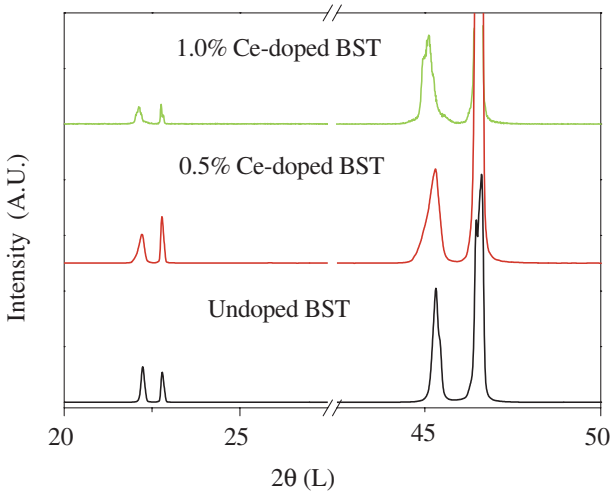


**Figure 1.** XRD pattern of undoped and Ce-doped BST films on Nb-doped $SrTiO_3$ substrate.

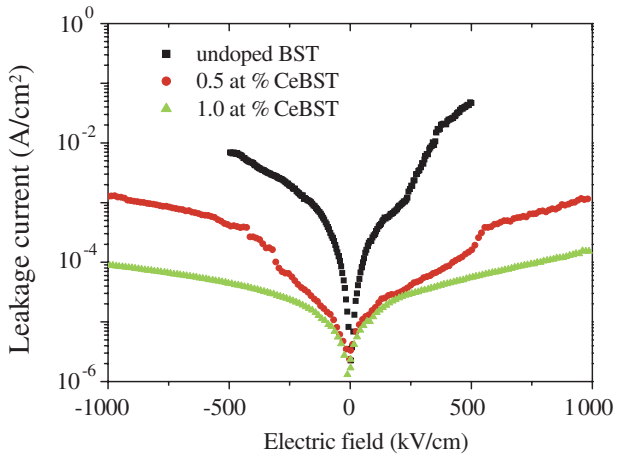


**Figure 2.** Variation of leakage current density as a function of bias electric field at room temperature for the undoped, 0.5 and 1.0 at% Ce-doped BST films.

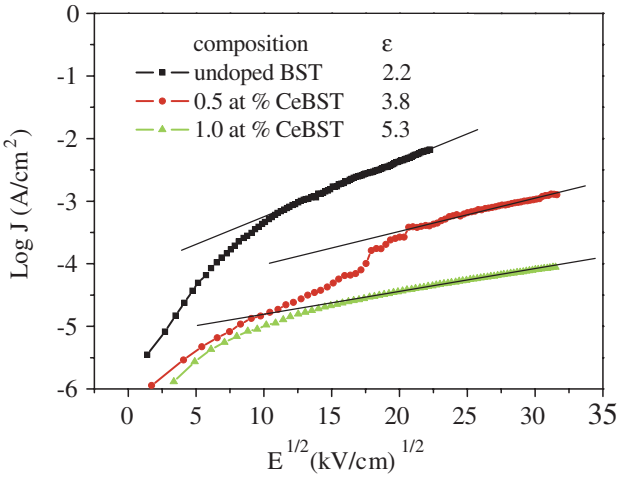


**Figure 3.** The log $J$ versus $E^{1/2}$ plot under negative bias electric field. The solid lines are used to fit the experimental data.

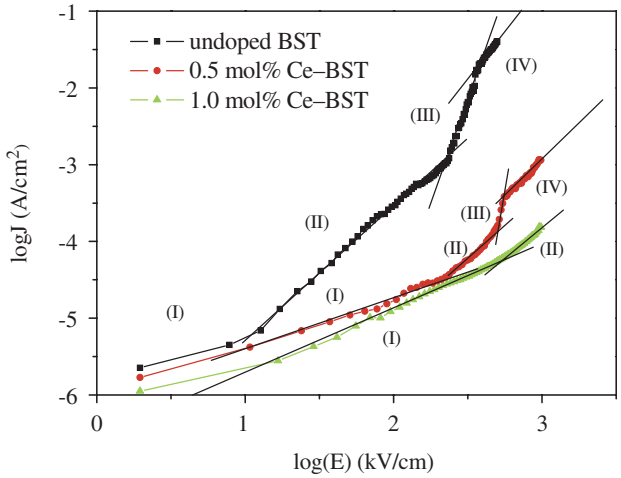


**Figure 4.** The plots of log($J$) versus log($V$) under positive bias of undoped, 0.5 at%, and 1.0 at% Ce-doped BST films at room temperature with solid indicating the slopes.

where $A^*$ is the Richardson constant, $T$ the absolute temperature, $E$ the applied electric field, $\Phi_B$ the Schottky barrier height at the Pt electrode, $q$ the electronic charge, $\varepsilon_0$ the permittivity of free space, $\varepsilon$ the optical dielectric constant and $k$ the Boltzmann constant. If the conduction current at high electric field is governed by Schottky emission, the log $J$ versus $E^{1/2}$ plot should be a straight line and the slope will give the optical dielectric constant. The optical dielectric constant of a BST thin film is 4.0, determined from an optically measured refractive index [14]. In figure 3, log $J$ is plotted versus $E^{1/2}$ for the leakage current data from the negative bias region. It can be seen that, for $E$ higher than a threshold value, the Schottky emission equation provides a good fit with the leakage current data, as indicated by the solid line. As shown in figure 3, the calculated optical dielectric constant is close to 4.0 in 0.5 and 1.0 at.% Ce-doped BST thin films and deviates from 4.0 in undoped BST thin films. So, at a high negative electric field, the leakage current data of Ce-doped BST thin films can be well described by the Schottky equation.

Plots of log ($J$) versus log ($E$) with various Ce concentrations, measured under positive electric field, are shown in figure 4. The curves clearly exhibit different slope regions for the $J$–$E$ characteristics. In the low bias region I, the slopes of the $J$–$E$ curves are all close to 1.0. With increasing electric fields, the slopes of the $J$–$E$ curve become about 2.0 (region II). At progressively higher electric fields a transition region is seen, characterized by a large slope (region III). At the highest positive bias electric field measured (region IV) the slopes of $J$–$E$ change to about 2.0 again. Such types of $J$–$E$ curves can be modelled in terms of a SCLC model with a discrete set of shallow traps [15, 16]. In regions I, II and IV, the deviations of the slope from the value of 1.0, 2.0 and 2.0, respectively, can be attributed to the scattered distribution of the trapping levels due to structural and chemical disorders in the thin films [15]. The transition electric field, $E_{\Omega\text{-SCL}}$, separating ohmic from space charge limited behaviour is given by [16]

$$E_{\Omega\text{-SCL}} = \frac{8qn_e d}{9\theta\varepsilon_r\varepsilon_0}. \tag{2}$$

A sharp increase in leakage current occurs at the so-called 'trap-filled limit' electric field ($E_{TFL}$), which can be expressed as [16]

$$E_{TFL} = \frac{8qdN_t}{9\varepsilon_r\varepsilon_0}. \tag{3}$$

In equations (2) and (3), $\theta$ is a constant, $n_e$ the electron density of the BST film, $\varepsilon_r$ the permittivity of BST film, $\varepsilon_0$ the permittivity of free space, $q$ the charge on an electron, $d$ the thickness of BST film and $N_t$ the concentration of shallow traps.

The transition electric field $E_{\Omega\text{-SCL}}$ between ohmic and space charge limited behaviour can be estimated from figure 4 as 10 kV cm$^{-1}$, 230 kV cm$^{-1}$ and 495 kV cm$^{-1}$ for undoped, 0.5 at%, and 1.0 at% Ce-doped BST films, respectively. The trap-filled limited electric field $E_{TFL}$ estimated from figure 4 is about 77 kV cm$^{-1}$ and 167 kV cm$^{-1}$ for the undoped and 0.5 at% for the Ce-doped BST film, respectively. For the 1.0 at% Ce-doped BST film (and upto 1000 kV cm$^{-1}$) we only see an ohmic region and a region displaying SCLC with traps: higher electric fields would be needed to see trap-free square law behaviour in this film. Furthermore, from the ratio of current jump $\theta$ in region III, the energy level of traps can be readily calculated from the following equation [16, 17].

$$\theta = \frac{n_f}{n_t} = \frac{N_c}{gN_t}\exp\left(\frac{-(E_c - E_t)}{kT}\right), \tag{4}$$

where $N_c$ is the effective density of states in the conduction band, $E_t$ the energy level of traps, $E_c$ the lower energy level of the conduction band, $g$ the degeneracy factor (∼2), $n_f$ the free electron concentration and $n_t$ the trapped electron concentration ($n_e = n_f + n_t$). In order to estimate the value of ($E_c - E_t$), $N_c$ is assumed to be $10^{21}$ cm$^{-3}$ [15]. The 0.5 at% Ce-doped BST film exhibited a lower value of ($E_c - E_t$) (0.20 eV) than the undoped BST film (0.27 eV).

The Ce-doping-induced reduction of leakage current in our BST film can be understood as follows. Usually the Ce ion can take two valence states: $Ce^{3+}$ and/or $Ce^{4+}$, depending on the processing condition. We suggest that at high temperature with low oxygen partial pressure, the Ce ion can be totally

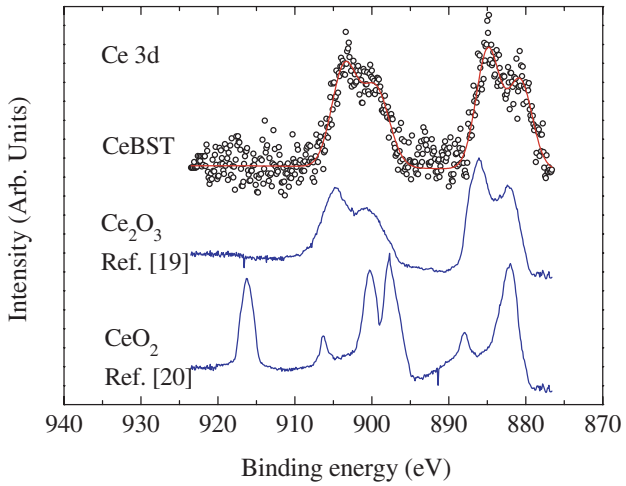


**Figure 5.** The Ce three-dimensional x-ray photoelectron core-level spectrum of Ce-doped BST film, compared with those of $Ce_2O_3$ (from [19]), and $CeO_2$ (from [20]).

reduced, and consequently it dissolves into BST as $Ce^{3+}$ [18]. In order to determine the valence state of the Ce ion in our Ce-doped-BST film, XPS measurements were carried out using Mg K$\alpha$ radiation ($h\nu = 1253.6$ eV). The binding energy was corrected with respect to the C 1s line at 284.6 eV. Figure 5 compares the Ce core-level spectra of Ce-doped BST with those of the formally trivalent $Ce_2O_3$, and the formally tetravalent $CeO_2$, which were reproduced from [19] and [20], respectively. The experimental data (dots) are fitted to the sum (solid line) of Gaussian functions. From figure 5 we see that our Ce 3D spectra are very similar to that of $Ce_2O_3$, although our Ce 3D core-level undergoes a shift to lower binding energy, which is probably due to the surface state and will be discussed in another paper. Furthermore, the highest binding energy peak centred at about 917 eV, which is observed for $CeO_2$ and is absent for $Ce_2O_3$, does not appear in our spectra. From the measured binding energy given by the XPS results, we find that Ce is trivalent and acts as an acceptor in Ce-doped BST films.

Just as in Co-acceptor doping of BST thin films [12], acceptor $Ce^{3+}$ replaces $Ti^{4+}$ in the BST lattice and a doubly ionized oxygen vacancy is simultaneously formed, i.e.

$$BaO(\text{or } SrO) + Ce_2O_3 \rightarrow Ba_{Ba}(\text{or } Sr_{Sr}) + 2Ce'_{Ti} + 4O_O + V_{\ddot{o}}, \quad (5)$$

where $V_{\ddot{o}}$ is an extrinsic oxygen vacancy controlled by the Ce content. At high deposition temperatures and lower oxygen partial pressure, BST thin films generally contain oxygen vacancies in the film according to [6]

$$O_o \leftrightarrow V_{\ddot{o}} + \tfrac{1}{2}O_2 + 2e', \quad (6)$$

where $O_o$ and $e'$ represent the oxygen ion on its normal site and free electron, respectively. From equations (5) and (6), it can be seen that the excess oxygen vacancies created by Ce addition can cause an inverse shift in reversible neutrality in equation (6) and eventually results in reduction of free electrons. In this way, Ce doping results in the decrease of electron concentration in BST thin films.

In the region of negative bias at the top electrode, the leakage current controlled by Pt/BST interface behaves in accordance with the Schottky emission model. The decrease of electron concentration can result in an increase of barrier height, as proposed by Copel *et al* [9]. They presented evidence, using XPS, that acceptor-doped films show an increased barrier to thermonic emission of electrons from the Pt contacts into the BST. The increased barrier height makes it difficult for electrons to transfer from the Pt electrode into the BST film. Thus, in the negative bias region the Ce-doped BST thin films exhibit lower leakage current than the undoped BST. In the positive bias region, the leakage current controlled by the STON/BST interface shows SCLC behaviour. The origin of the reduction of leakage current is similar to that of acceptor Co-doping [12]. In the low positive bias region, the decreased electron concentration and carrier mobility lower the leakage current; in the high positive bias region, the decreased value of $(E_c\text{-}E_t)$ for the traps associated with Ce-doping is responsible for the reduction of the leakage current.

## 4. Summary

In conclusion, Ce-doping has been shown to be an effective way of decreasing the leakage current in a Pt/BST/STON capacitor in both the positive and negative bias regions. Ce is trivalent in Ce-doped BST film, as determined by the XPS measurement. In the positive bias region, the leakage mechanism shows SCLC behaviour at room temperature, the transition electric field $E_{\Omega\text{-SCL}}$ and trap-filled limit electric field are both increased with Ce addition. In the negative bias region, the leakage current is dominated by Schottky emission, and Ce-doping increases the barrier height, which is likely to be responsible for the reduction of the leakage current in the BST thin films.

## Acknowledgments

The authors are very grateful for the support of the 'Hundreds Talents Project' of the Chinese Academy of Sciences and the National Natural Science Foundation of China.

## References

[1] Jia Q X, Park B H, Gibbons B J, Huang J Y and Lu P 2003 *Appl. Phys. Lett.* **81** 114
[2] Tao K, Hao Z, Xu B, Chen B, Miao J, Yang H and Zhao B R 2003 *J. Appl. Phys.* **94** 4042
[3] Yang H, Chen B, Tao K, Qiu X G, Xu B and Zhao B R 2003 *Appl. Phys. Lett.* **83** 1611
[4] Ahn K H, Baik S and Kim S S 2002 *J. Appl. Phys.* **92** 2651
[5] Im J, Streiffer S K, Auciello O and Krauss A R 2000 *Appl. Phys. Lett.* **77** 2593
[6] Sze S M 1981 *Physics of Semiconductor Devices* 2nd edn (New York: Wiley)
[7] Lee J S, Li Y, Lin Y, Lee S Y and Jia Q X 2004 *Appl. Phys. Lett.* **84** 3825
[8] Hwang C S *et al* 1998 *J. Appl. Phys.* **83** 3703
[9] Copel M, Baniecki J D, Duncombe P R, Kotecki D, Laibowitz R, Neumayer D A and Shaw T M 1998 *Appl. Phys. Lett.* **73** 1832
[10] Sedlar M, Saver M and Weaver L 1995 *J. Sol–Gel Sci. Tech.* **5** 201
[11] Sedlar M, Saver M and Weaver L 1995 *Integrated Ferroelectrics* **10** 113

[12] Wang S Y, Cheng B L, Wang C, Dai S Y, Lu H B, Zhou Y L, Chen Z H and Yang G Z 2004 *Appl. Phys. Lett.* **84** 4116
[13] Wang S Y, Cheng B L, Wang C, Dai S Y, Lu H B, Zhou Y L, Chen Z H and Yang G Z 2004 *Appl. Phys. A: Mater. Sci. Process.* at press
[14] Shimada Y *et al* 1996 *Japan. J. Appl. Phys.* (part 1) **35** 140
[15] Peng C J and Krupanidhi S B 1995 *J. Mater. Res.* **10** 708
[16] Lampert M A and Mark P 1970 *Current Injection in Solids* (New York: Academic)
[17] Chang S T and Lee J Y M 2002 *Appl. Phys. Lett.* **80** 655
[18] Makovec D and Kolar D 1997 *J. Am. Ceram. Soc.* **80** 45
[19] Allen J W 1985 *J. Magn. Magn. Mater.* **47/48** 168
[20] Wuilloud E, Delley B, Schneider W D and Baer Y 1984 *Phys. Rev. Lett.* **53** 202